Appendix

A Privacy Analysis

We analyze the security of GCFGAE under the semi-honest model [Brickell and Shmatikov, 2005], that is, all participants and the coordinator strictly follow the procedure of GCFGAE and never collude with others to peek at any participant's privacy. Specifically, we examine each step of GCFGAE's training to ensure that no graph privacy defined in subsection 3.2 is breached.

Before the stage of Laplace matrix construction, the PSI protocol was used by each participant in pairs to match the overlapping vertices $V_{k,ov}$ between them. According to the proof [De Cristofaro and Tsudik, 2010], PSI protocol can ensure that no participant can decrypt the other participant's local vertices from the encrypted information received, thus ensuring the security of each participant's local private data.

In the stage of Laplacian matrix construction, the intermediate data transmitted between participants and the coordinator includes $\mathbf{D}_{k,ov}$ and $\mathbf{D}_{c,ov}$. The former is encrypted by secret sharing. The latter is the sum of all $\mathbf{D}_{k,ov}$s from which no one can deduce $\mathbf{D}_{k,ov}$ unless only one participant is in model training, which is impractical. Therefore , the Laplacian matrix construction is secure under the semi-honest model.

During the forward propagation of GCFGAE, the intermediate data transmitted between participants and the coordinator in steps 1 and 2 is the initial weight matrices $\mathbf{W}^{(0)} \sim \mathbf{W}^{(L-1)}$ which contain no participant's graph privacy. In steps 3 and 4, $\mathbf{H}_{k,ov}^{(0)}$ and $S_{k,ov}$ are sent from each participant to the coordinator. First, they are encrypted by secret sharing. Second, $S_{k,ov}$ includes only the intermediate terms in the computation of the embedding vectors of overlapping vertices. Therefore, steps 3 and 4 do not compromise the privacy of any participant. In step 5, a participant can deduce no information about other participants' overlapping vertices from $\mathbf{H}_{k,ov}^{(0)}$ unless only two participants are involved in model training, a situation that is rarely encountered in the real world. Furthermore, according to the analysis in [Chen *et al.*, 2021; Duddu *et al.*, 2020], a participant cannot deduce any raw information of other participants from the embedding vectors transmitting between participants and the coordinator without auxiliary information such as a participant's subgraph. Therefore, step 5 is secure under the semi-honest adversary assumption. In steps 6 and 7, the intermediate data transmitted between participants and the coordinator is $\mathbf{H}_k^{(L-1)'}$. It does not disclose any participant's graph privacy for the same reason as step 5. The reconstructed $\hat{\mathbf{A}} \neq \mathbf{A}$ so the coordinator is unaware of the true topology of each participant's local graph. In summary, the forward propagation of GCFGAE is secure against semi-honest adversaries.

During the backward propagation of GCFGAE, the intermediate data transmitted between participants and the coordinator in steps 1 and 2 includes $\left(\left(\frac{\partial \hat{\mathbf{A}}}{\partial \mathbf{H}^{(L-1)}}\right)_k\right)_i$ and $\langle \frac{\partial \mathcal{L}_k}{\partial \mathbf{H}^{(L-1)}} \rangle$. The former is only a partial term in equation 7 for the computation of $\frac{\partial \mathcal{L}_k}{\partial \mathbf{H}^{(L-1)}}$. Since another term $\left(\frac{\partial \mathcal{L}_k}{\partial \hat{\mathbf{A}}_k}\right)_i$ in equation 7 is computed by each participant locally, an adversary is unable to infer gradient matrix $\frac{\partial \mathcal{L}_k}{\partial \mathbf{H}^{(L-1)}}$ even he has the plain text of $\left(\left(\frac{\partial \hat{\mathbf{A}}}{\partial \mathbf{H}^{(L-1)}}\right)_k\right)_i$. The latter is encrypted by secret sharing. Therefore, Steps 1 and 2 leak no participant's graph privacy. The intermediate data sent by the coordinator to each participant in step 3 is the $\left(\frac{\partial \mathcal{L}}{\partial \mathbf{H}^{(L-1)}}\right)_k$ corresponding to participant P_k and extracted from $\left(\frac{\partial \mathcal{L}}{\partial \mathbf{H}^{(L-1)}}\right)$. According to equation 8, $\left(\frac{\partial \mathcal{L}}{\partial \mathbf{H}^{(L-1)}}\right)$ is computed based on three terms where $\frac{\partial \mathcal{L}_k}{\partial \mathbf{H}^{(L-1)}}$ is in ciphertext. Therefore, it is impossible for the coordinator or any adversary to obtain any participant's $\langle \frac{\partial \mathcal{L}_k}{\partial \mathbf{H}^{(L-1)}} \rangle$. In step 4, the $\left(\frac{\partial \mathcal{L}}{\partial \mathbf{W}^{(L-1)}}\right)_k$ sent by each participant to the coordinator is encrypted by secret sharing. In step 5, no participant can deduce other participant's $\left(\frac{\partial \mathcal{L}}{\partial \mathbf{W}^{(L-1)}}\right)_k$ from the sum $\left(\frac{\partial \mathcal{L}}{\partial \mathbf{W}^{(L-1)}}\right)$. Step 6 is executed by each participant locally. Therefore, the three steps bear no privacy leakage. The intermediate data transmitted between participants and the coordinator in steps 7 and 8 is the encrypted $\langle (\frac{\partial \mathcal{L}_k}{\partial \mathbf{H}^{(L-2)}})_{ov} \rangle$. Hence, it discloses no participant's graph privacy. Step 9 is conducted locally. In summary, the backward propagation of GCFGAE is also secure against semi-honest adversaries.

From the above analysis, we conclude that GCFGAE can protect the graph privacy of all participants under the semi-honest model.

B Consistency Analysis

We verify the consistency between GCFGAE and the centralized GAE step by step.

PSI protocol can make each participant know the overlap-

ping vertices $V_{k,ov}$ based on protecting the local privacy of the participant to construct the Laplacian matrix in the following steps. PSI protocol is used in the data preprocessing stage and does not affect the correctness of subsequent algorithms.

In the stage of Laplacian matrix construction, under the scenario of horizontal federated graph learning shown in Figure 1, participants share overlapping vertices but no overlapping links. Therefore, the $\mathbf{D}_{c,ov}$ computed in steps 1 and 2 through the collaboration of participants and the coordinator is complete for overlapping vertices and contains no redundant term. Secret sharing does not affect the correctness of the computation. In step 3, because participants share only overlapping vertices but not overlapping links, the Laplacian matrix $\tilde{\mathbf{A}}_{nov}$ encoding the adjacency relationships between two participants' non-overlapping vertices is a zero matrix, that is, $\tilde{\mathbf{A}}_{nov} = [0]$. Therefore, the local degree matrices $\mathbf{D}'_k$s form a complete global degree matrix $\mathbf{D}$ when they are placed in their correct positions in $\mathbf{D}$, that is, $\mathbf{D} = ||\mathbf{D}'_k$. Furthermore, when all local Laplacian matrices $\tilde{\mathbf{A}}_k$s computed based on $\mathbf{D}_{k,ov}$s and $\mathbf{D}'_k$s are combined with $\tilde{\mathbf{A}}_{nov}$, we have $\left(||\tilde{\mathbf{A}}_k\right) ||\tilde{\mathbf{A}}_{nov} = ||\tilde{\mathbf{A}}_k = \tilde{\mathbf{A}}$. Consequently, the Laplacian matrices computed by GCFGAE and the centralized GAE are identical.

During the forward propagation of GCFGAE, all participants share the same weight matrices $\mathbf{W}^{(0)} \sim \mathbf{W}^{(L-1)}$. In step 1, the local first-layered embedding matrix $\mathbf{H}_k^{(0)}$ is computed according to the same equation 1 as the centralized GAE. In steps 2 to 5, first, the part in $\mathbf{H}_k^{(0)}$ corresponding to non-overlapping vertices, denoted as $\mathbf{H}_{k,nov}^{(0)}$, is equivalent to that in the centralized GAE's $\mathbf{H}^{(0)}$ because there is no links between each participant's non-overlapping vertices and between a participant's overlapping vertices and any other participant's non-overlapping vertices in the scenario of horizontal federated graph learning. Second, for the overlapping vertices, the local embedding matrix $\mathbf{H}_{k,ov}^{(0)}$ of each participant is correctly constructed, given that set $S_{k,ov}$ correctly records the duplicated terms in the computation of overlapping vertices' embedding vectors and these terms are correctly deduced according to equation 5 in step 4. In other words, the embedding vectors in $\mathbf{H}_{k,ov}^{(0)}$ are identical to those computed for the overlapping vertices in the centralized GAE. Therefore, the embedding vectors in $\mathbf{H}_k^{(0)'}$ are equivalent to those corresponding to the same vertices in participant P_k in the first-layered embedding matrix $\mathbf{H}^{(0)}$ computed by the centralized GAE. The same conclusion applies to the computation of $\mathbf{H}_{k,ov}^{(1)}$ to $\mathbf{H}_{k,ov}^{(L-2)}$. In step 6, the local reconstructed adjacency matrix $\hat{\mathbf{A}}_k$ is computed according to the same equation as that used for computing $\hat{\mathbf{A}}$ in the centralized GAE. In step 7, the embedding vectors in $\mathbf{H}^{(L-1)'}$ which is constructed by combining all $\mathbf{H}_k^{(L-1)'}$ are equivalent to those computed in the centralized GAE for the same reason stated above. The global loss$\mathcal{L}$ is not directly computed, but its gradients with respect to embedding and weight matrices are computed in the backward propagation and are proved to be correct in the next paragraph. In summary, the forward propagation of GCFGAE is consistent with that of the centralized GAE.

During the backward propagation of GCFGAE, the gradients of the global loss $\mathcal{L}$ with respect to the $(L-1)$th-layered embedding matrix $\mathbf{H}^{(L-1)}$, as shown in equation 8, is computed according to the chain rule of matrix calculus in steps 1 to 3. The direct computation of $\frac{\partial \mathcal{L}}{\partial \mathbf{H}^{(L-1)}} = \sum_k \frac{\partial \mathcal{L}_k}{\partial \mathbf{H}^{(L-1)}}$ overcounts the gradients of $\mathcal{L}$ with respect to the embedding vectors of overlapping vertices in $\mathbf{H}^{(L-1)}$. Therefore, by subtracting $\sum_i \left(\left(\frac{\partial \mathcal{L}}{\partial \hat{\mathbf{A}}_{ov}}\right)_i \left(\frac{\partial \hat{\mathbf{A}}_{ov}}{\partial \mathbf{H}^{(L-1)}}\right)_i\right)$ from them, we can deduct the duplicated terms from the sum. Additionally, the gradients of $\mathcal{L}$ with respect to the embedding vectors of non-overlapping vertices, that is, $\sum_i \left(\left(\frac{\partial \mathcal{L}}{\partial \hat{\mathbf{A}}_{nov}}\right)_i \left(\frac{\partial \hat{\mathbf{A}}_{nov}}{\partial \mathbf{H}^{(L-1)}}\right)_i\right)$, should be appended. The complex computation is used to ensure that the $\frac{\partial \mathcal{L}}{\partial \mathbf{H}^{(L-1)}}$ computed by GCFGAE is equivalent to that computed by the centralized GAE. In steps 4 to 6, the gradients of the global loss $\mathcal{L}$ with respect to the $(L-1)$th-layered weight matrix $\mathbf{W}^{(L-1)}$ computed according to equations 9 and 10 is equivalent to that computed by the centralized GAE because only one global $\mathbf{W}^{(L-1)}$ is shared between all participants. In steps 7 to 8, the equivalence between the gradients $\left(\frac{\partial \mathcal{L}}{\partial \mathbf{H}^{(L-2)}}\right)_{c,ov}$ computed by GCFGAE for the $(L-2)$th-layered embedding vectors of overlapping vertices and that computed by the centralized GAE is guaranteed by selecting and aggregating the proper gradients in $\left(\frac{\partial \mathcal{L}}{\partial \mathbf{W}^{(L-1)}}\right)_k$ according to the chain rule. In step 9, since $\left(\frac{\partial \mathcal{L}}{\partial \mathbf{H}^{(L-2)}}\right)_{c,ov}$ is properly computed and the correctness of steps 4 to 6 is explained above, the computation of $\left(\frac{\partial \mathcal{L}}{\partial \mathbf{W}^{(L-2)}}\right)$ by GCFGAE is equivalent to that computed by the centralized GAE. In summary, the backward propagation of GCFGAE is consistent with that of the centralized GAE.

From the above analysis, we conclude that GCFGAE is consistent with the centralized GAE in federated graph model training.

C Communication and Space Complexity

The communication complexity of the Laplacian matrix construction is $O(\sum_k n_{k,ov})$, where $n_{k,ov}$ is the number of overlapping vertices of participant P_k, which is spent on the transmission of degree matrices $\mathbf{D}_{k,ov}$s. The intermediate data transmitted during the forward propagation includes the embedding matrices $\mathbf{H}_k^{(l)}$, $\langle \mathbf{H}_{k,ov}^{(l)} \rangle$, $\mathbf{H}_{c,ov}^{(l)}$ and $\mathbf{H}_k^{(0)'}$ of each layer l. Therefore, the communication complexity of the forward propagation is $O(I_r \sum_k (d_e n_{k,ov} L + n_k d_e))$, where n_k is the number of vertices of participant P_k's local graph, d_e is the dimension of a vertex's embedding vector, I_r is the number of iterations, L is the number of layers in GCFGAE. The communication complexity of the forward propagation is linear to the number of overlapping vertices rather than the total number of vertices of a participant's local graph. The communication complexity of the backward propagation is $O\left((\sum_k (n_k^2 d_e + n_k d_e + n_{k,ov} d_e L) + n_W L) I_r\right)$, where n_W is the number of elements of the weight

matrix $\mathbf{W}$. The complexity is quadratic to the total number of vertices of a participant's local graph because some gradient matrices transmitted between participants and the coordinator, such as $\left(\frac{\partial \mathcal{L}}{\partial \mathbf{W}^{(L-1)}}\right)_k$, is in the size of $O(n_k^2)$. The overall communication complexity of GCFGAE is $O(I_r \sum_k (d_e n_{k,ov} L + n_k d_e) + (\sum_k (n_k^2 d_e + n_k d_e + n_{k,ov} d_e L) + n_W L) I_r)$, which can be reduced to $O(n^2)$ where $n = \sum_k n_k$ is the sum of the number of vertices in all participants' graphs because $d_e, L, I_r << n$ and $n_k, n_{k,ov}, n_W < n$.

The space complexity of the Laplacian matrix construction is $O(\sum_k (n_k^2 + n_k d_e))$, which is used to store the adjacency matrix $\tilde{\mathbf{A}}_k$ and the attribute matrix $\mathbf{X}_k$ of participant P_k. The space complexity of the forward propagation of GCFGAE is $O(\sum_k (n_k^2 + n_k d + L n_w + L n_k d_e + L n_{k,ov} d_e) + n^2)$, which is used to store the adjacency matrix $\tilde{\mathbf{A}}_k$, attribute matrix $\mathbf{X}_k$, parameter matrix $\mathbf{W}_k$ and embedding matrix $\mathbf{H}_k$ of participant P_k and the duplicated term set $S_{k,ov}$ and the global reconstructed matrix $\hat{\mathbf{A}}$. The space complexity of the backward propagation is $O(n^2 + n d_e + \sum_k (n_k^2 + n d_e) + \sum_k (L n_k d_e) + \sum_k (n_k^2 + n_k d + L n_w) + \sum_k (L n_k d_e))$, which is used to store the global reconstructed matrix $\hat{\mathbf{A}}$, the global embedding matrix $\mathbf{H}^{(l)}$ and the matrices $\frac{\partial \mathcal{L}_k}{\partial \mathbf{H}^{(l)}}$ and $\left(\frac{\partial \mathcal{L}}{\partial \mathbf{H}^{(l)}}\right)_k$ computed by participant P_k for the lth layer, and the weight matrix $\mathbf{W}_k$ in participant P_k. Therefore, the overall space complexity of GCFGAE is $O(n^2 + n d_e + \sum_k (n_k^2 + n_k d + L n_w + L n_k d_e + L n_k d_e + n d_e))$, which can be reduced to $O(n^2)$ because $d_e, L << n$ and $n_k, n_W < n$.

D Experimental Results

We provide the raw data for the bar chart in the paper. Table 1 shows the original NMI values and ARI values of the consistency experiment, in which the NMI values and ARI values of 2 to 10 participants are the same. Table 2 and Table 3 show the original NMI values of the accuracy experiment results of each algorithm with 2 participants and 10 participants. Table 4 and Table 5 show the original NMI values on the Amazon and Lastfm datasets with the number of participants varying from 2 to 10. Table 6 shows the original CO values and SO values of the communication experiments and space overhead experiments.We show the experimental results on training time and convergence rate under the 2 participant settings in Figure **??**.

Table 1: NMI and ARI of the consistency experiment

Datasets	GCFGAE		GAE	
	NMI	ARI	NMI	ARI
Cora	0.5409	0.4640	0.5409	0.4640
Citeseer	0.2538	0.1668	0.2538	0.1668
Amazon	0.8856	0.8011	0.8856	0.8011
DBLP	0.4045	0.3215	0.4045	0.3215
Lastfm	0.6134	0.5772	0.6134	0.5772

Table 2: NMI of the accuracy experiment (2 participants)

Datasets	GCFGAE	SAPGNN	Fedavg+GAE	SDGAE
Cora	0.5409	0.2396	0.3143	0.2357
Citeseer	0.2538	0.1725	0.1449	0.1418
Amazon	0.8856	0.6501	0.7974	0.6244
DBLP	0.4045	0.2108	0.2995	0.2064
Lastfm	0.6134	0.3125	0.5357	0.3087

Table 3: NMI of the accuracy experiment (10 participants)

Datasets	GCFGAE	SAPGNN	Fedavg+GAE	SDGAE
Cora	0.5409	0.0511	0.3552	0.1405
Citeseer	0.2538	0.0658	0.1994	0.0562
Amazon	0.8856	0.3494	0.6516	0.2350
DBLP	0.4045	0.1439	0.2832	0.0339
Lastfm	0.6134	0.2251	0.4657	0.2021

Table 4: NMI of the accuracy experiment on Amazon

Number of participants	GCFGAE	SAPGNN	Fedavg+GAE	SDGAE
2	0.8856	0.6501	0.7974	0.6244
4	0.8856	0.5271	0.7484	0.4062
6	0.8856	0.4443	0.7023	0.3113
8	0.8856	0.3556	0.6799	0.2361
10	0.8856	0.3494	0.6516	0.2350

Table 5: NMI of the accuracy experiment on Lastfm

Number of participants	GCFGAE	SAPGNN	Fedavg+GAE	SDGAE
2	0.6134	0.3125	0.5357	0.3087
4	0.6134	0.2779	0.4992	0.2623
6	0.6134	0.2625	0.4846	0.2538
8	0.6134	0.2510	0.4695	0.2297
10	0.6134	0.2251	0.4657	0.2021

Table 6: Results of the communication and space overhead experiment

Datasets	GCFGAE				SAPGNN			
	CO(lg MB)		SO(lg MB)		CO(lg MB)		SO(lg MB)	
	2	10	2	10	2	10	2	10
Cora	5.96	5.36	3.37	3.36	8.73	8.16	6.75	6.62
Citeseer	6.07	5.41	3.45	3.42	8.75	8.19	6.90	6.77
Amazon	5.69	5.01	3.34	3.32	8.49	7.64	6.56	6.42
DBLP	5.40	4.74	3.33	3.31	8.15	7.45	6.44	6.31
Lastfm	5.17	4.83	3.32	3.31	8.06	7.65	6.06	5.96

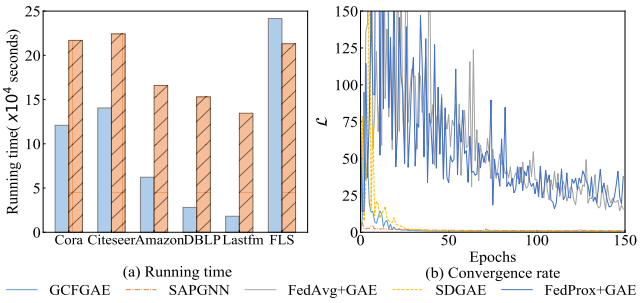

Figure 1: Running time and convergence rate of the models

References

[Brickell and Shmatikov, 2005] Justin Brickell and Vitaly Shmatikov. Privacy-preserving graph algorithms in the semi-honest model. In *Advances in Cryptology-ASIACRYPT 2005: 11th International Conference on the Theory and Application of Cryptology and Information Security, Chennai, India, December 4-8, 2005. Proceedings 11*, pages 236–252. Springer, 2005.

[Chen *et al.*, 2021] Fahao Chen, Peng Li, Toshiaki Miyazaki, and Celimuge Wu. Fedgraph: Federated graph learning with intelligent sampling. *IEEE Transactions on Parallel and Distributed Systems*, 33(8):1775–1786, 2021.

[De Cristofaro and Tsudik, 2010] Emiliano De Cristofaro and Gene Tsudik. Practical private set intersection protocols with linear complexity. In *Financial Cryptography and Data Security: 14th International Conference, FC 2010, Tenerife, Canary Islands, January 25-28, 2010, Revised Selected Papers 14*, pages 143–159. Springer, 2010.

[Duddu *et al.*, 2020] Vasisht Duddu, Antoine Boutet, and Virat Shejwalkar. Quantifying privacy leakage in graph embedding. In *MobiQuitous 2020-17th EAI International Conference on Mobile and Ubiquitous Systems: Computing, Networking and Services*, pages 76–85, 2020.